Materials Chemistry and Physics 119 (2010) 237–242

Contents lists available at ScienceDirect

Materials Chemistry and Physics

journal homepage: www.elsevier.com/locate/matchemphys

Poly (vinyl alcohol) thin film filled with CdSe–ZnS quantum dots: Fabrication, characterization and optical properties

Baoting Suo[a], Xin Su[b], Ji Wu[b], Daniel Chen[a], Andrew Wang[c], Zhanhu Guo[a,*]

[a] Integrated Composites Laboratory (ICL), Dan F. Smith Department of Chemical Engineering, Lamar University, Beaumont, TX 77710, USA
[b] Department of Chemical and Materials Engineering, University of Kentucky, Lexington, KY 40506, USA
[c] Ocean NanoTech, LLC, 2143 Worth Ln., Springdale, AR 72764, USA

ARTICLE INFO

Article history:
Received 2 April 2009
Received in revised form 10 June 2009
Accepted 25 August 2009

Keywords:
Composite materials
Optical materials
Optical properties
Quantum dots

ABSTRACT

A transparent poly (vinyl alcohol) (PVA) nanocomposite thin film (30–50 nm) reinforced with core/shell cadmium selenide (CdSe)/zinc sulfide (ZnS) quantum dots (QDs) was fabricated by a drop-casting method. A narrow peak at ~556 nm observed in the UV–vis spectrum indicates the uniformly dispersed QDs in the PVA matrix. FT-IR analysis indicates the interaction between the QDs and the polymer matrix. Both PVA and PVA-QDs nanocomposite thin films show polarized light dependent absorption properties with several different absorption peaks. As compared to the only fluorescent emission peak at 574 nm of QDs, the pure PVA and PVA-DDs nanocomposites show an excitation wavelength dependent fluorescent emission property.

1. Introduction

Fluorescent organic and inorganic materials are promising in studying the complexity and dynamics of biological process [1,2]. The physicochemical properties will change radically as the materials evolve from the bulk level to the atomic or molecular counterparts [3]. Compared to the traditional dyes (fluorescent organic molecules), semiconductive nanocrystals have broader excitation wavelength range, narrower and tunable emission spectra [1], more resistant to chemicals and metabolic degradation, and higher photobleaching threshold [4–6]. Nanocrystals with controllable solubility and shape can be accurately synthesized by judiciously controlling the reaction conditions [7–9]. These nanocrystals have attracted much interest due to their wide potential engineering applications such as biology and medication, biological fluorescence labeling and imaging [2,10,11]. The prominent focus has been the optical properties, showing a strong size-dependent quantum confinement effect [2,7,12,13]. The quantum confinement effect takes place when the quantum well thickness becomes comparable to the de Broglie wavelength of the carriers (generally electrons and holes), leading to energy levels called "energy subbands". In other words, the wavelength is inversely proportional to the momentum of a particle and the frequency is directly proportional to the particle's kinetic energy. The electrons and holes in a semiconductor are confined by a potential well when at least one dimension approaches the size of an electron in bulk crystal [14]. Moreover, the emission pattern can be narrow and independent of the excitation frequency, even though the absorption spectrum is a continuum from infrared to UV [2].

Colloidal nanocrystals or nanoparticles tend to aggregate in solution due to their large surface energy. To stabilize nanomaterials, various stabilizers (surfactants, polymers or coupling agents) have been employed to modify the surface functionalities for obtaining stable nanocrystals [11]. Cadmium selenide (CdSe) quantum dots (QDs) have attracted considerable attention arising from their unique optical properties, including extended optical absorption in the ultra-violet region, bright photoluminescence (PL), narrow emission band, size tunable PL and photostability [13,15–18], and their potential promising PL materials for optical electronic device applications [19–21].

CdSe quantum dot growth includes a two-dimensional (2d) wetting layer and a given critical thickness of a few layers of three-dimensional (3d) islands shape, which is called the self-organized Stranski-Krastanov growth (SK growth) mode. These processes are probably accelerated by a nonuniform strain distribution and nonequilibrium growth conditions, which produce anomalously high density of cation vacancies [22,23]. In the PL, these defects act as a trap for the excited electrons and holes [24]. The energy required for adding additional charges to a semiconductor particle varies inversely with the increase of the particle size. One of the most striking properties is the massive optical properties change as a function of size. As the particle size decreases, the electronic excitations shift to higher energy. For a free particle, both energy and crystal momentum can be precisely defined, whereas the posi-

* Corresponding author. Tel.: +1 409 880 7654.
E-mail address: zhanhu.guo@lamar.edu (Z. Guo).

0254-0584/$ – see front matter © 2009 Elsevier B.V. All rights reserved.
doi:10.1016/j.matchemphys.2009.08.054

tion cannot. However, in a localized particle, the energy rather than position and momentum may be well defined. The discrete energy fluctuation can be viewed as superpositions of particle momentum states [16]. The shifts of absorption in CdSe colloidal aqueous solution can be a large fraction of the bulk band gap and can result in tuning across a major portion of the visible spectrum. The band gap in CdSe can be tuned from deep red (1.7 eV) to green (2.4 eV) by reducing the cluster diameter from 20 nm to 2 nm [17]. All of these properties make CdSe attractive for biological application. Because of the toxicity of heavy metal cadmium, the CdSe QDs are coated with a biocompatible zinc sulfide (ZnS) layer, with a matching crystal lattice constant to minimize the defects. For the solubility in water, the surface of the QDs is coated with carboxyl groups.

Polymer nanocomposites have attracted much interest due to their unique physicochemical properties and wide potential applications [25–29]. In addition, the presence of quantum dots or nanoparticles in the solid polymer matrix will prevent the nanoparticle agglomeration and make the nanoparticles storage easier as compared to the colloidal counterparts. In this project, poly (vinyl alcohol) (PVA) is chosen as hosting materials in the composite fabrication due to its polar and hydrophilic properties, good thermo-stability, chemical resistance, easy processability and transparency [30].

In this paper, a transparent poly (vinyl alcohol) (PVA) nanocomposites filled with semiconductive CdSe/ZnS quantum dots were fabricated by a drop-casting method. Transmission electron microscopy (TEM) and high-resolution TEM show uniform size and highly crystallized quantum dots. The interaction between the quantum dots and polymer matrix was indicated by Fourier transform infrared (FT-IR) spectrophotometer analysis. The optical absorption and fluorescent emission properties of the polymer nanocomposites were investigated by UV–vis spectrophotometer and fluorescence spectrophotometer, respectively, and compared with those of the pure PVA and QDs. Polarized lights were found to have significant effect on the absorption performance. PVA-QDs nanocomposites excited by different wavelength show different fluorescent behaviors.

2. Experimental

2.1. Materials

Poly (vinyl alcohol) (PVA, MW = 88,000–96,800, degree of polymerization 2000–2200) was purchased from Sigma–Aldrich Company. CdSe–ZnS quantum dots coated with organic molecules containing carboxyl groups were supplied by Ocean Nanotechnology Company. All the chemicals were used as-received without further treatment.

2.2. Thin film fabrication

2.2.1. Pure PVA thin film fabrication

The PVA thin film was prepared as follows. White PVA powder (5 g, 0.11 mol) was dissolved in de-ionized water (95 g). After a 2-h magnetic stirring at 50 °C, 10 wt% transparent PVA aqueous solution was formed. The PVA thin film was formed by dropping 3–5 ml PVA aqueous solution onto a 12-cm diameter Petri dish and drying in an oven at 60 °C for 10 h.

2.2.2. PVA-QDs nanocomposite thin film fabrication

2.5 ml QDs aqueous solution (3 g quantum dots per 100 g solution) was added into PVA aqueous solution. The PVA-QDs nanocomposite thin film was made following the same procedures as those used for the pure PVA thin film fabrication. The typical film thickness was measured to be 30–50 μm.

2.3. Characterization

The morphology (size and shape) of CdSe–ZnS quantum dots was characterized in a JEOL 2010F transmission electron microscopy (TEM) with an accelerating voltage of 200 keV. The samples were prepared by dropping aqueous quantum dots solution onto a holey carbon coated copper grid and drying naturally in air.

Energy dispersive X-ray spectroscopy (EDAX) (attached to a Hitachi S-3400 scanning electron microscopy) was used to characterize the elemental composition of the quantum dots. The sample was prepared by dropping 1 ml quantum dots solution on a piece of aluminum foil and drying at 50 °C for 10 h. The orange residue was further tested by Fourier transform infrared spectroscopy (FT-IR, a Bruker Inc. Tensor 27 FT-IR spectrometer with hyperion 1000 ATR microscopy accessory) to characterize the surface chemistry of the quantum dots. Both PVA thin film and PVA-QDs nanocomposite thin films were characterized by FT-IR to investigate the interaction between the nanoparticles and the polymer matrix.

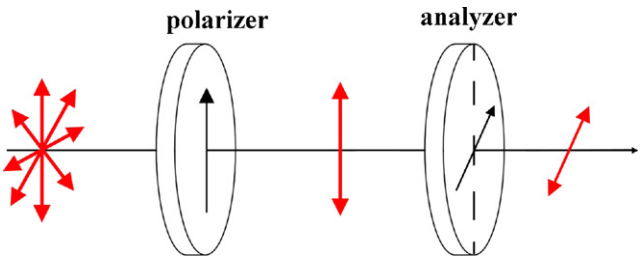

Fig. 1. Diagram of malus law, a normal light travelled from left to right, through a polarizer and an analyzer.

The CdSe–ZnS quantum dots aqueous solution was tested by a Cary 50 bio ultraviolet–visible (UV–vis) spectrophotometer. Because of the strong UV absorption, the QDs solution was diluted to 5–10% of its original concentration and put in a standard 10 mm path length cuvette for UV–vis test. Both PVA and PVA-QDs nanocomposite thin films were tested by polarized beams at different directions and conducted in a UV–vis spectrophotometer. A polarizer (Tiffen 49 mm) was placed between the light source and the sample, parallel to the sample. A filter was rotated per measurement with a fixed angle at ~6° perpendicular to the direction of the beam. Polarized light passed through pure PVA thin film and PVA-QDs nanocomposite thin films and absorption spectra were obtained. Polarized beams vibrate perpendicularly to the direction and travel with a beam pattern period of 180°. The beams have been polarized before passing through the PVA thin film. Based on Malus's law [31], $I(\theta) = I_0 \times \cos^2(\theta)$, where I_0 is the initial intensity and $I(\theta)$ is the intensity after passing the polarizer. θ is the angle of a polaroid analyzer, which is placed with respect to the polarizer, as schematically shown in Fig. 1. According to Malus's law, the period of the polarized beams was reduced to 90°.

Photoluminescence (PL) spectra of all the samples were recorded at room temperature and measured by a Varian CARY Eclipse fluorescence spectrophotometer. The liquid sample was diluted to be 5–10% of its original concentration and contained in a standard 10 mm path length cuvette for fluorescence test. The nanocomposite thin films with a dimension of 10 mm × 40 mm were used for both UV–vis and fluorescence tests.

3. Results and discussion

Fig. 2(a) shows the TEM microstructure of the as-received CdSe–ZnS quantum dots. No obvious aggregation was observed in the samples and the average particle size was 3.5 nm with a standard deviation of 0.7 nm. Fig. 2(b) shows the high-resolution TEM microstructure of the CdSe–ZnS quantum dots. Well-resolved lattice fringes were observed continuously throughout an entire single particle, indicating a highly crystalline (nanocrystal) structure of the quantum dots. The lattice spacing was calculated to be 0.37 nm, 0.25 nm and 0.31 nm, which corresponded to (1 0 0) and (1 0 2) CdSe crystal planes and (1 0 2) ZnS crystal plane, respectively. No clear interface between CdSe core and ZnS shell was observed in the analyzed quantum dots, indicating an epitaxial growth of the crystal shell [32].

The composition of core–shell CdSe–ZnS quantum dots coated with carboxyl groups was examined by an energy dispersive X-ray spectroscopy (EDAX) and FT-IR. The EDAX analysis, Fig. 3(a), showed elements of carbon, oxygen, sulfur, cadmium, zinc, and selenium, consistent with the provided components of the quantum dots. Carbon and oxygen could be from the used substrate or the carboxyl groups. The surface functional groups are further characterized by FT-IR spectrophotometer. Fig. 3(b) shows the FT-IR spectra of the dried CdSe–ZnS QDs. The characteristic stretch peaks of C–H (2914 and 2820 cm^{-1}) [33] and –COOH (1697 and 1398 cm^{-1}) [34] were observed. Peaks at 1050 cm^{-1} may represent C–C group. This was consistent with the provided information that quantum dots are coated with surfactant having carboxyl groups.

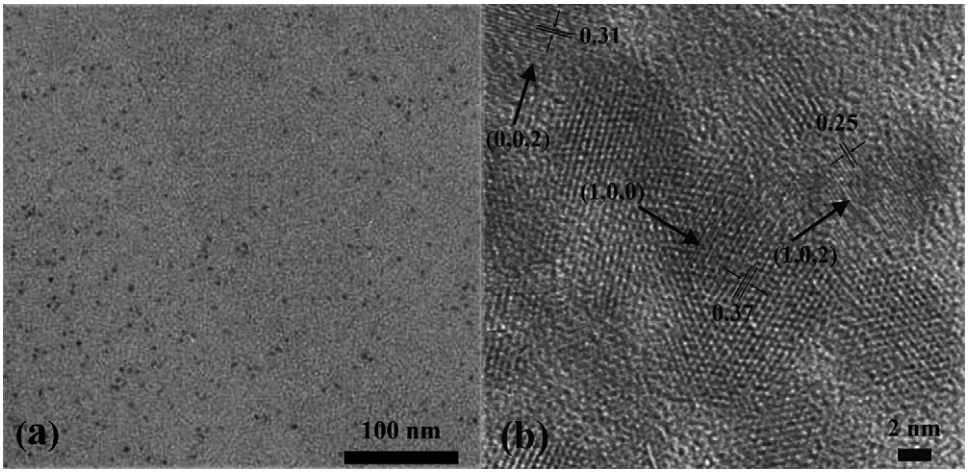

Fig. 2. (a) TEM microstructure and (b) HRTEM microstructure of as-received quantum dots.

Fig. 4 shows the FT-IR spectra of the dried QDs, pure PVA thin film, and PVA-QD nanocomposite thin film, respectively. All the samples have characteristic C–H stretch peaks [33] at 670 and 2914 cm^{-1}, and $-CH_2$ stretch peaks at 1320 cm^{-1}. The peaks showed stronger intensity in the dried QDs samples and weaker in the polymer nanocomposites. The peak of 2820 cm^{-1} was exhibited in the composites, which was absent in the pure PVA sample. Both –OH stretch peaks [35,36] (3285 and 1650 cm^{-1}), C–C stretch peaks [37] (1413 cm^{-1}) and C–O stretch peaks [37] (850, 1167 and 1390 cm^{-1}) were found stronger in both PVA and nanocomposites, and weaker in the evaporated QDs sample. On the polymer chain of PVA, hydroxyl groups were linked to the carbon chain. The QDs sample has a weak response to –OH group through the hydrogen bondage. A strong –COOH stretch peak [34] at 1735 cm^{-1} was observed in dried QDs sample, not seen in pure PVA. These differences indicate an interaction between the quantum dots and polymer matrix.

Fig. 5 shows the UV–vis absorption spectra of CdSe–ZnS quantum dots aqueous solution, pure PVA thin film, and PVA-QDs nanocomposite thin film, respectively. PVA thin film showed little absorption. The quantum dots solution showed an onset at 556 nm, corresponding to absorption energy of 2.24 eV ($\nu = c/\lambda$, $E = h \times \nu$, ν is light wave frequency, s^{-1}; c is light speed, 3×10^8 m s^{-1}; λ is wavelength, m; E is wave energy, eV; h is Planck's constant, 4.135×10^{-15} eV s). The measured 2.24 eV showed a blue shift, relative to the band gap (E_g) of the bulk cubic CdSe (1.77 eV) [38], which may be attributed to the small size or the effect of ZnS shell. The estimated E_g of CdSe was based on the measured wavelength of approximately one-third of the main absorption feature [39]. The composite showed a peak at the same position of the quantum dots aqueous solution. The absorption decreased with the increase of the wavelengths in both composite and aqueous QDs solution. The strong band-edge absorption indicates the potential applications of these nanocomposites in optoelectronic device areas.

The energy band gap of PVA-QDs nanocomposite is determined by the reflection spectrum. According to Tauc relation, $\alpha h\nu = A \times (h\nu - E_g)^n$, where α is the absorption coefficient, $h\nu$ is the energy of a photon, A is a constant, varies according to ele-

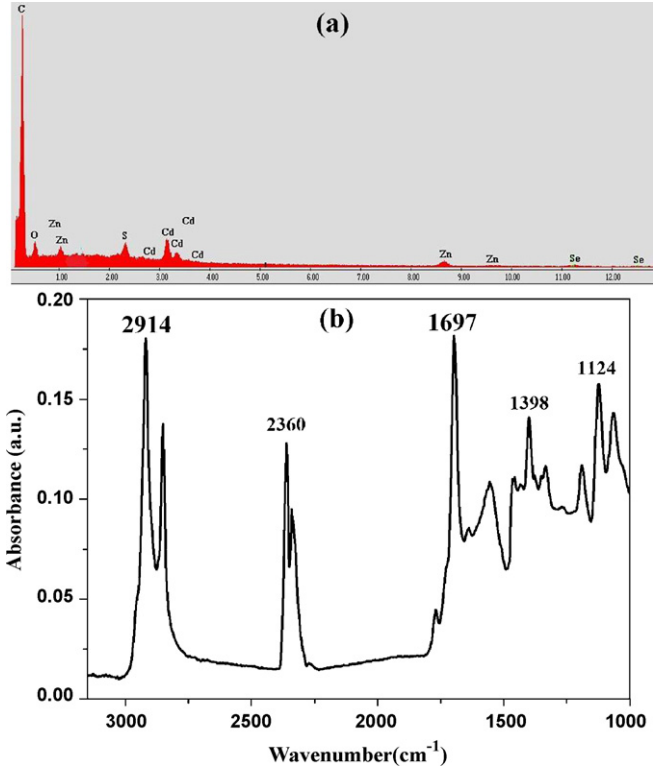

Fig. 3. (a) EDAX image of evaporated QDs, and (b) FT-IR image of as-received QDs after complete drying.

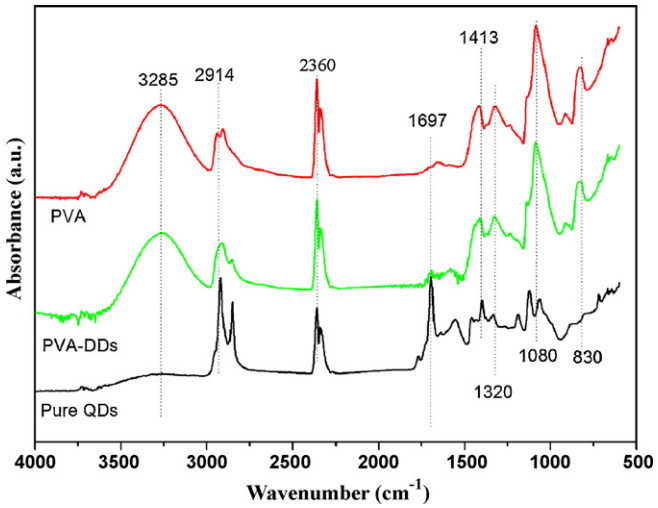

Fig. 4. FT-IR spectra of PVA thin film, PVA-QDs thin film composite and evaporated CdSe–ZnS QDs.

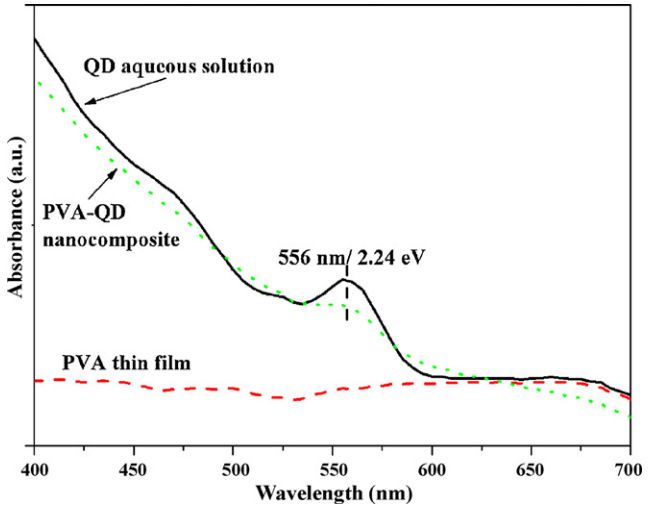

Fig. 5. UV–vis absorption of QDs aqueous solution, pure PVA thin film and PVA-QDs nanocomposite.

ments, E_g is the energy gap of CdSe and n is an index depending on the nature of the electronic transition responsible for the reflection. Reflection, R, is obtained from $R = 1/(10^A)$, where A is absorbance value. Absorption coefficient α has the following relation: $2\alpha t = \ln[(R_{max} - R_{min})/(R - R_{min})]$, where t is the thickness of the sample. R_{max} and R_{min} are the maximum and minimum values of reflection. Fig. 6 is to determine the index n using a graph of $\ln\{h\nu \times \ln[(R_{max} - R_{min})/(R - R_{min})]\}$ vs $\ln(h\nu - E_g)$ [40]. The energy gap for CdSe is 1.74 eV [41]. The slope of the line is 2.6. Fig. 6 is got by using $\{h\nu \times \ln[(R_{max} - R_{min})/(R - R_{min})]\}^{2.6}$ vs energy. The extrapolation of the straight line to $h\nu \times \ln[(R_{max} - R_{min})/(R - R_{min})] = 0$ gives the value of band gap of PVA-QDs nanocomposite. According to the graph, the band gap value is 2.80 eV for PVA-QDs nanocomposite. The change of band gap suggests the structural change occurring in the nanocomposite or the ZnS shell effect.

Fig. 7 shows the UV–vis absorption spectra of pure PVA thin film with the polarizer rotated for one full cycle. Based on Malus's law, the period of the polarized beams was 90° as schematically shown in the experiment. Five absorption peaks at around 380 nm, 470 nm, 525 nm, 695 nm and 785 nm were observed. A shift of absorption peaks was detected with the change of polarized beams. Within the observed wavelength range of 350–700 nm, the absorption peak in the top curve gradually increased as compared to the bottom

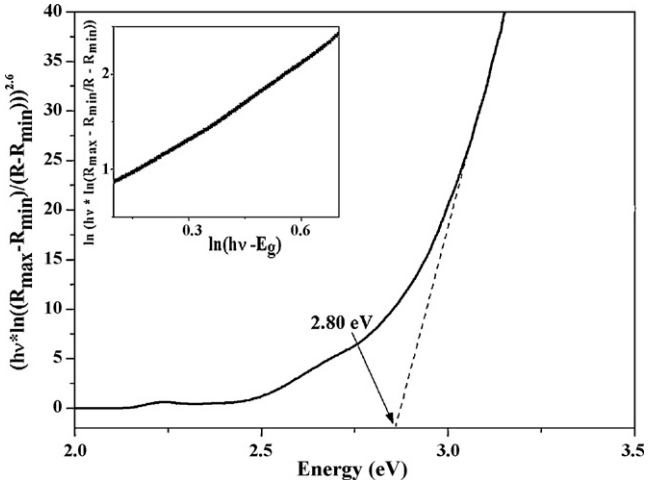

Fig. 6. Using UV–vis absorption to determine the band gap of PVA-QDs nanocomposites.

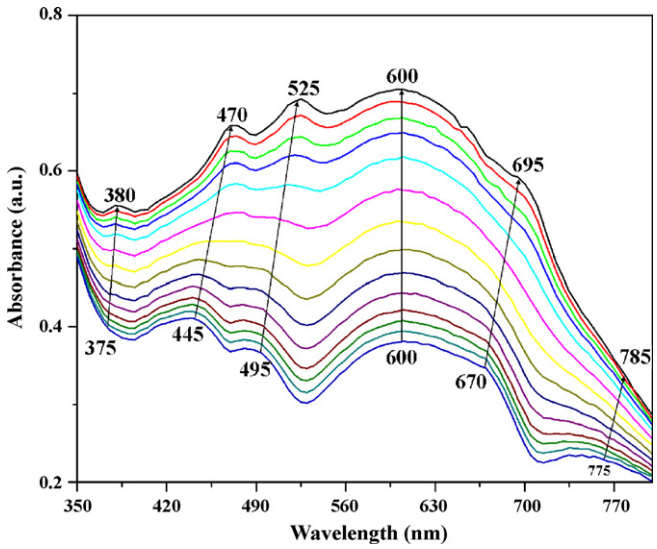

Fig. 7. UV–vis absorption spectra of PVA thin film with polarizer 90°-rotated.

curve. For example, a shoulder was observed in the bottom curve for the wavelength range of 370–390 nm and a well-resolved absorption peak was observed in the top curves. At about 600 nm, there was little absorption change with the change of polarized beams. In the wavelength range of 720–770 nm, the absorption decreases sharply for the curves at top and there is an absorption plateau in the bottom curves. In addition, an absorption peak was observed the bottom curves. These indicate that the optical absorption was influenced by the polarized lights passing through the transparent PVA. The absorbance of PVA thin film was observed 0.3–0.7 in the range of 350–700 nm. A shoulder at about 770 nm and the overall sharp absorption decreased were observed.

Fig. 8 shows the UV–vis absorption spectrum of nanocomposite thin film measured by the same procedures as in Fig. 7. The spectra can be approximated by the superposition of the spectra of PVA thin film and QDs solution. Additional features and variations were observed. The absorbance of the nanocomposite thin film mainly lies between 0.45 and 0.90 from 400 nm to 700 nm. A new peak at 563 nm was observed in the nanocomposite thin film [38], which resembles the peak of CdSe–ZnS QDs. The nanocomposites showed the absorption peaks at 470 nm, 520 nm, 700 nm

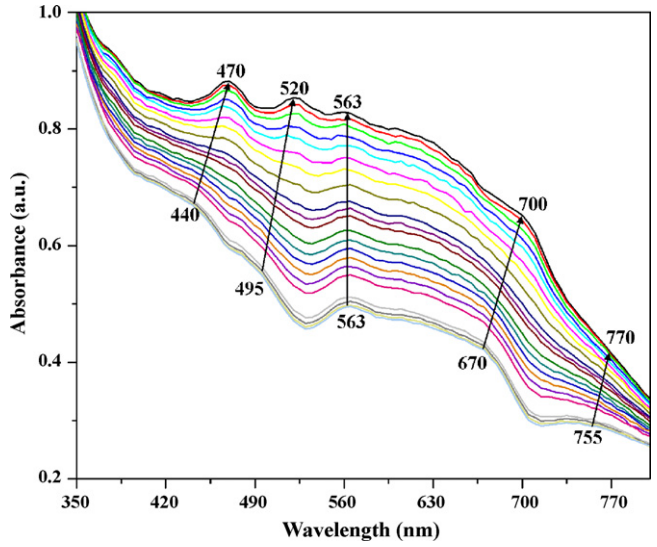

Fig. 8. UV–vis absorption spectra of composite thin film with polarizer 90°-rotated.

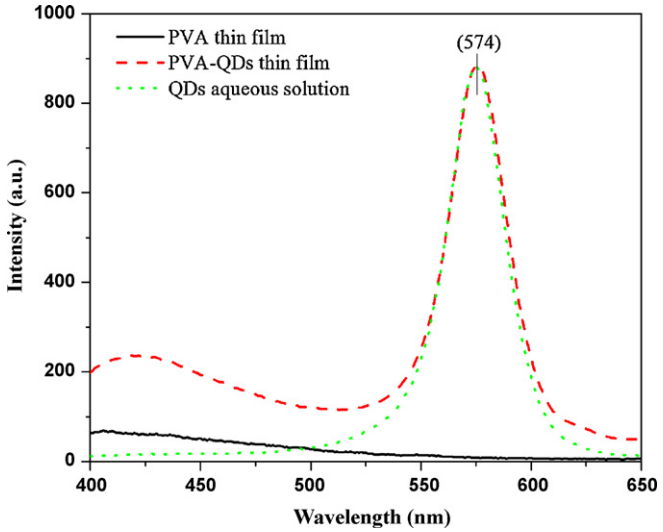

Fig. 9. Fluorescence spectra of QDs aqueous solution, PVA thin film and PVA-QDs composite.

and 770 nm, similar to those of the pure PVA. The peak at 600 nm became weaker compared to that of the pure PVA. The spectrum difference indicates the influence of QDs and an interaction between the QDs and the PVA polymer matrix, consistent with the FT-IR analysis.

Fig. 9 shows the fluorescence spectra of QDs aqueous solution, pure PVA thin film and PVA-QD nanocomposite thin film, respectively. The excitation wavelength was 350 nm. A peak at 574 nm was observed in both QDs aqueous solution and PVA-QD nanocomposite thin film, which was characteristic of CdSe quantum dots [42]. No fluorescence phenomenon was observed in pure PVA thin film in the observed wavelength ranging from 400 nm to 650 nm.

Fig. 10 shows the fluorescence spectra of QDs, excited by beams of selected wavelengths from 260 nm to 288 nm. A significant increase in fluorescent emission intensity was observed. The huge increase was found by a small change of the excitation wavelength (less than 30 nm). The fluorescent peaks of QDs and the corresponding polymer nanocomposites were observed to be located at the wavelength of 574 nm.

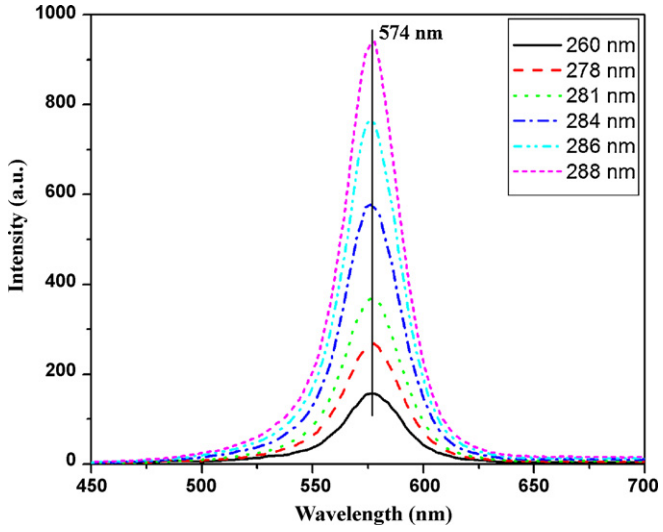

Fig. 10. Fluorescence spectra of QDs aqueous solution excited by different wavelength.

4. Conclusion

Uniform CdSe–ZnS quantum dots functionalized with carboxyl groups on the surface were used to prepare PVA-QDs nanocomposite thin film by drop-casting method. FT-IR spectra of the nanocomposite indicate the interaction between the QDs and the polymer matrix. With the aid of UV–vis spectrophotometer, the polymer composites showed absorption at 563 nm, similar to the pure QDs solution. The nanocomposites showed a compromised absorption of the polymer and the nanosized fillers. The composites have also shown special optical absorption property when subjected to polarized beams in UV–vis test. During fluorescence test, a stable emission peak for QDs and a shifting peak for PVA were observed. With transparent biodegradable PVA as base material, nanocomposites reinforced with QDs have great potential optical electronic applications. With the fluorescent quantum dots as nanofillers, these nanocomposites have great potential applications in the biomedical area.

Acknowledgements

This project is partially supported by Northrop Grumman Corporation. Great support from the research start-up fund of Lamar University was kindly acknowledged. B. Suo also expresses his appreciation for the generous scholarship from the Dan F. Smith Department of Chemical Engineering at Lamar University to conduct this project.

References

[1] J. Riegler, F. Ditengou, K. Palme, T. Nann, J. Nanobiotechnol. 6 (2008) 7.
[2] D. Gerion, F. Pinaud, S. Williams, W. Parak, D. Zanchet, S. Weiss, A. Alivisatos, J. Phys. Chem. B 105 (2001) 8861–8871.
[3] V. Biju, Y. Makita, A. Sonoda, H. Yokoyama, Y. Baba, M. Ishikawa, J. Phys. Chem. B 109 (2005) 13899–13905.
[4] M. Bruchez Jr., M. Moronne, P. Gin, S. Weiss, A.P. Alivisatos, Science 281 (1998) 2013–2016.
[5] W.C.W. Chan, S. Nie, Science 281 (1998) 2016–2018.
[6] J. Jaiswal, H. Mattoussi, J. Mauro, S. Simon, Nat. Biotechnol. 21 (2003) 47–51.
[7] L. Manna, E.C. Scher, A.P. Alivisatos, J. Am Chem. Soc. 122 (2000) 12700–12706.
[8] J.J. Welser, S. Tiwari, S. Rishton, K.Y. Lee, Y. Lee, IEEE Electron Device Lett. 18 (1997) 278–280.
[9] C.B. Murray, C.R. Kagan, M.G. Bawendi, Science 270 (1995) 1335–1338.
[10] J. Gao, B. Xu, Nano Today 4 (2008) 37–51.
[11] (a) M.K. Patra, M. Manoth, V.K. Singh, G.S. Gowd, V.S. Choudhry, S.R. Vadera, N. Kumar, J. Lumin. 129 (2008) 320–324;
(b) Z. Guo, C. Kumar, L.L. Henry, E.E. Domes, J. Hormes, E.J. Podlaha, J. Electrochem. Soc. 152 (1) (2005) D1–D5;
(c) Z. Guo, L.L. Henry, V. Palshin, E.J. Podlaha, J. Mater. Chem. 16 (2006) 1772–1777;
(d) Z. Guo, T. Pereira, O. Choi, Y. Wang, Hahn HT, J. Mater. Chem. 16 (2006) 2800–2808.
[12] A.L. Efros, M. Rosen, Annu. Rev. Mater. Sci. 30 (2000) 475–521.
[13] M. Nirmal, L. Brus, Acc. Chem. Res. 32 (1999) 407–414.
[14] K.E. Andersen, C.Y. Fong, W.E. Pickett, J. Non-Cryst. Solids 299–302 (2002) 1105–1110.
[15] A.P. Alivisatos, J. Phys. Chem. 100 (1996) 13226–13239.
[16] A.P. Alivisatos, Science 271 (1996) 933–937.
[17] C.B. Murrary, C.R. Kagan, M.G. Bawendi, Annu. Rev. Mater. Sci. 30 (2000) 545–610.
[18] B.O. Dabbousi, J. Rodriguez-Viejo, F.V. Mikulec, J.R. Heine, H. Mattoussi, R. Ober, K.F. Jensen, M.G. Bawendi, J. Phys. Chem. B 101 (1997) 9463–9475.
[19] S. Chaudhary, M. Ozkan, W.C.W. Chan, Appl. Phys. Lett. 84 (2004) 2925–2927.
[20] D. Klein, R. Roth, A. Lim, A.P. Alivisatos, P.L. McEuen, Nature 389 (1997) 699–701.
[21] G.W. Walker, V.C. Sundar, C.M. Rudzinski, A.W. Wun, M.G. Bawendi, D.G. Nocera, Appl. Phys. Lett. 83 (2003) 3555–3557.
[22] P.D. Thang, G. Rijnders, D.H.A. Blank, J. Magn. Magn. Mater. 310 (2007) 2621–2623.
[23] Z.H. Hua, R.S. Chen, C.L. Li, S.G. Yang, M. Lu, B.X. Gu, Y.W. Du, J. Alloys Compd. 427 (2007) 199–203.
[24] V.V. Strelchuk, M.Y. Valakh, M.V. Vuychik, S.V. Ivanov, P.S. Kop'ev, T.V. Shubina, Semicond. Phys., Quant. Electron. Optoelectron. 5 (2002) 343–346.
[25] Z. Guo, K. Lei, Y. Li, H.W. Ng, H.T. Hahn, Compos. Sci. Technol. 68 (2008) 1513–1520.
[26] Z. Guo, S. Wei, B. Shedd, R. Scaffaro, T. Pereira, H.T. Hahn, J. Mater. Chem. 17 (2007) 806–813.

[27] S. Lee, H.-J. Shin, S.-M. Yoon, D.K. Yi, J.-Y. Choi, U. Paik, J. Mater. Chem. 18 (2008) 1751–1755.
[28] Y. Chen, L. Sun, O. Chiparus, I. Negulescu, V. Yachmenev, M. Warnock, J. Polym. Environ. 13 (2005) 107–114.
[29] Z. Guo, S. Park, H.T. Hahn, S. Wei, M. Moldovan, A.B. Karki, D.P. Young, Appl. Phys. Lett. 90 (2007) 053111.
[30] S. Liu, J. He, J. Xue, W. Ding, J. Nanopart. Res. 11 (2009) 553–560.
[31] C. Brukner, A. Zeilinger, Acta Phys. Slovaca 49 (1999) 647–652.
[32] S. Schinzer, M. Sokolowski, M. Biehl, W. Kinzel, Surf. Sci. 1–3 (1999) 191–198.
[33] Deschenaux Ch, A. Affolter, D. Magni, Ch. Hollenstein, P. Fayet, J. Phys. D: Appl. Phys. 32 (1999) 1876–1886.
[34] P. Hellwiq, B. Rost, U. Kaiser, C. Ostermeier, H. Michel, W. Mantele, FEBS Lett. 385 (1996) 53–57.
[35] S. Matveev, M. Portnyagin, C. Ballhaus, R. Brooker, C.A. Geiger, J. Petrol. 46 (2005) 603–614.
[36] D. Okuno, T. Iwase, K. Shinzawa-Itoh, S. Yoshikawa, T. Kitagawa, J. Am. Chem. Soc. 125 (2003) 7209–7218.
[37] X.M. Sui, C.L. Shao, Y.C. Liu, Appl. Phys. Lett. 87 (2005) 113–115.
[38] A. Pan, H. Yang, R. Liu, R. Yu, B. Zou, Z. Wang, J. Am. Chem. Soc. 127 (2005) 15692–15693.
[39] O. Palchik, R. Kerner, A. Gedanken, A.M. Weiss, M.A. Slifkin, V. Palchik, J. Mater. Chem. 11 (2001) 874–878.
[40] G.P. Joshi, N.S. Saxena, R. Mangal, A. Mishra, T.P. Sharma, Band gap determination of Ni–Zn ferrites, Bull. Mater. Sci. 26 (2003) 387–389.
[41] W.C. Kwak, T.G. Kim, W.S. Chae, Y.M. Sung, Tuning the energy band gap of CdSe nanocrystals via Mg doping, Nanotechnology 18 (2007) 205702.
[42] H. Mattoussi, A.W. Cumming, C.B. Murray, M.G. Bawendi, R. Ober, Phys. Rev. B: Condens. Matter 58 (1998) 7850–7863.